



Contents lists available at ScienceDirect

Steroids

journal homepage: www.elsevier.com/locate/steroids

Discovery of a novel isoxazoline derivative of prednisolone endowed with a robust anti-inflammatory profile and suitable for topical pulmonary administration

E. Ghidini^{a,*}, A.M. Capelli^a, C. Carnini^c, V. Cenacchi^b, G. Marchini^c, A. Viridis^d, A. Italia^e, F. Facchinetti^c^a Chemistry Research and Drug Design Department, Chiesi Farmaceutici S.p.A., Parma, Italy^b Pharmacokinetic Department, Chiesi Farmaceutici S.p.A., Parma, Italy^c Pharmacology and Toxicology Department, Chiesi Farmaceutici S.p.A., Parma, Italy^d Nikem Research Srl, Baranzate di Bollate (Mi), Italy^e Chimani Srl, via Reggio Calabria, 12 Rottofreno (PC), Italy

ARTICLE INFO

ABSTRACT

Q4 Article history:

Received 4 June 2014

Received in revised form 27 November 2014

Accepted 15 December 2014

Available online xxxxx

Keywords:

Corticosteroid

Isoxazoline

Ovalbumin

Nuclear translocation

PK profile

GILZ

A novel glucocorticoids series of (GCs), 6 α ,9 α -di-Fluoro 3-substituted C-16,17-isoxazolines was designed, synthesised and their structure–activity relationship was evaluated with glucocorticoid receptor (GR) binding studies together with GR nuclear translocation cell-based assays. This strategy, coupled with *in silico* modelling analysis, allowed for the identification of Cpd #15, an isoxazoline showing a sub-nanomolar inhibitory potency (IC₅₀ = 0.84 nM) against TNF α -evoked IL-8 release in primary human airways smooth muscle cells. In Raw264.7 mouse macrophages, Cpd #15 inhibited LPS-induced NO release with a potency (IC₅₀ = 6 nM) > 10-fold higher with respect to Dexamethasone. Upon intratracheal (i.t.) administration, Cpd #15, at 0.1 μ mol/kg significantly inhibited and at 1 μ mol/kg fully counteracted eosinophilic infiltration in a model of allergen-induced pulmonary inflammation in rats. Moreover, Cpd #15 proved to be suitable for pulmonary topical administration given its sustained lung retention ($t_{1/2}$ = 6.5 h) and high pulmonary levels (>100-fold higher than plasma levels) upon intratracheal administration in rats. In summary, Cpd #15 displays a pharmacokinetic and pharmacodynamic profile suitable for topical treatment of conditions associated with pulmonary inflammation such as asthma and COPD.

© 2015 Published by Elsevier Inc.

1. Introduction

An important limitation of GCs therapy is that the desired anti-inflammatory effects are accompanied by side effects such as loss of muscle mass, redistribution of body fat, osteoporosis, diabetes, glaucoma and depression [1]. In patients with asthma and chronic obstructive pulmonary disease (COPD), the adverse effects of GCs chronic use can be limited by topical pulmonary delivery via inhalation [2]. Nevertheless, a degree of systemic exposure inevitably occurs which may raise safety concerns in elderly patients as well as in patients requiring high dose regimen [3]. Hence, there is the need to enhance local anti-inflammatory potency of topical GCs while limiting their systemic exposure in order to minimize unwanted side effects.

A considerable amount of research is aimed at discovering novel steroidal GR agonists with high anti-inflammatory potency upon topical application and limited systemic exposure. Despite these efforts, only few novel steroidal molecules showing significant structural changes with respect to existing drugs have been developed [4,5]. The present study attempts to fill this gap by describing the design, synthesis and pharmacological profile of a novel series of 6 α ,9 α -di-Fluoro 3-substituted isoxazolines. Cpd #15, in particular, proved to be a suitable compound for pulmonary topical administration given its robust anti-inflammatory potency, prolonged lung retention and low systemic exposure upon intratracheal administration.

2. Experimental section

2.1. Chemicals and reagents

All commercially available chemicals and solvents were purchased from Aldrich-Sigma (St. Louis, MO). Steroidal derivatives

Abbreviations: GCs, glucocorticoids; NO, nitric oxide; GILZ, glucocorticoid-induced leucine zipper; ASMCs, airway smooth muscle cells.

* Corresponding author. Tel.: +39 0521 279913; fax: +39 05212762 545567.

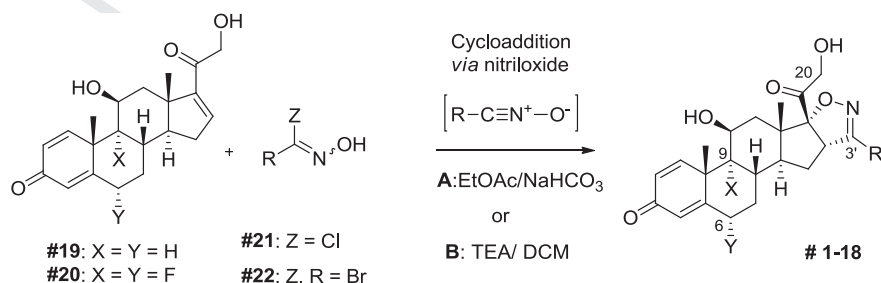
E-mail address: e.ghidini@chiesi.com (E. Ghidini).

(compounds **#1–18**) were synthesized in our laboratory following the route described in **Scheme 1**. Starting from commercially available derivative **#21** and for **#22**, the reaction proceeded in ethyl acetate and NaHCO₃, together with a few drops of water, by stirring at room temperature for six days (**Scheme 1**; A). When derivatives Cpd **#21** were prepared by *in situ* chlorination of the corresponding aldoximes with BTMAICl₄ (benzyltrimethylammonium tetrachloroiodate) [6] or bleach, the reaction proceeded in dry dichloromethane (DCM) and triethylamine (TEA) at room temperature for 3 h (**Scheme 1**; B). All reactions details are reported in the **Supporting Information**. The structures of these compounds are shown in **Table 1** and the steroidal drugs are:

(16S,17R)-3'-(4-chlorophenyl)-11β,21-dihydroxy-4'H-pregna-1,4-dieno[16,17-d]isoxazole-3,20-dione, Cpd **#1**; (16S,17R)-3'-(4-methoxyphenyl)-11β,21-dihydroxy-4'H-pregna-1,4-dieno[16,17-d]isoxazole-3,20-dione, Cpd **#4**; (16S,17R)-3'-methylacetate-11β,21-dihydroxy-4'H-pregna-1,4-dieno[16,17-d]isoxazole-3,20-dione, Cpd **#5**; (16S,17R)-3'-propyl-11β,21-dihydroxy-4'H-pregna-1,4-dieno[16,17-d]isoxazole-3,20-dione, Cpd **#6**; (16S,17R)-3'-methyl-11β,21-dihydroxy-4'H-pregna-1,4-dieno[16,17-d]isoxazole-3,20-dione, Cpd **#7**; (16S,17R)-3'-(hydroxymethyl)-11β,21-dihydroxy-4'H-pregna-1,4-dieno[16,17-d]isoxazole-3,20-dione, Cpd **#8**; (16S,17R)-3'-hydroxy-11β,21-dihydroxy-4'H-pregna-1,4-dieno[16,17-d]isoxazole-3,20-dione, Cpd **#10**; (16S,17R)-3'-(thiophen-3-yl)-11β,21-dihydroxy-4'H-pregna-1,4-dieno[16,17-d]isoxazole-3,20-dione, Cpd **#11**; (16S,17R)-3'-(furan-3-yl)-11β,21-dihydroxy-4'H-pregna-1,4-dieno[16,17-d]isoxazole-3,20-dione, Cpd **#12**; (16S,17R)-3'-(thiophen-3-yl)-6,9-difluoro-11β,21-dihydroxy-4'H-pregna-1,4-dieno[16,17-d]isoxazole-3,20-dione, Cpd **#13**; (16S,17R)-3'-(furan-3-yl)-6,9-difluoro-11β,21-

Table 1
Compounds series.

Compound	R	X, Y
#1	p-Cl-Phenyl,	H, H
#2	COOEt	H, H
#3	COOH	H, H
#4	p-OMe-Phenyl	H, H
#5	CH ₂ OCOCH ₃	H, H
#6	Propyl	H, H
#7	Methyl	H, H
#8	CH ₂ OH	H, H
#9	Br	H, H
#10	OH	H, H
#11	3-Thienyl	H, H
#12	3-Furyl	H, H
#13	3-Thienyl	F, F
#14	3-Furyl	F, F
#15	Br	F, F
#16	Methyl	F, F
#17	p-OMe-Phenyl	F, F
#18	Phenyl	F, F



Scheme 1. Compounds **1–18** were synthesized starting from enone, **#19** or **#20** and hydroximoyl chlorides derivatives **#21** or hydroxycarbonimidic dibromide **#22** via 1,3-dipolar cycloaddition of nitrile oxides.

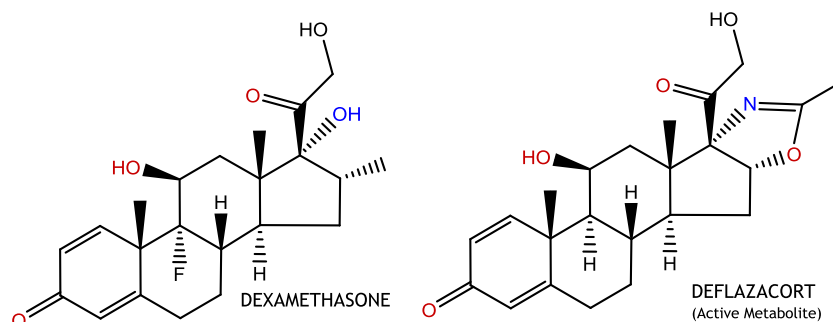


Chart 1.

Q5

156 samples were reacted with 1% sulfanilamide, 0.1% naphthyl
157 ethylenediamine dihydrochloride, and 2.5% phosphoric acid at
158 room temperature for 10 min, and nitrite concentration was deter-
159 mined by absorbance at 540 nm in comparison with sodium nitrite
160 as a standard. Compound potencies were expressed as concentra-
161 tion able to inhibit the half maximal (50%) NO release [IC₅₀] in
162 the dose–response curve obtained after stimulation with LPS.

163 2.2.3. Glucocorticoid receptor (GR) and mineralcorticoid receptor (MR) 164 translocation assay protocol

165 The cell-based GR-translocation assay in Enzyme Fragment
166 Complementation format developed by DiscoverRx (Fremont, CA)
167 was employed to quantitatively measure GR nuclear translocation
168 [9]. PathHunter CHO-K1 GR and PathHunter CHO-K1 MR cells were
169 seeded in a 96-well plate at 15,000 cells/well in 100 μL medium
170 without antibiotics and 24 hours later the compounds were added
171 (concentration ranging from 10⁻¹²M to 10⁻⁶M) for 3 h at 37 °C.
172 Luminescence, estimated as relative light units (RLU), was detected
173 by using a CENTRO LB 960 microplate reader (Berthold Technolo-
174 gies). Statistical analysis and determinations of EC₅₀s were per-
175 formed by using Prism-version 3.0 Graphpad Software (San
176 Diego, CA).

177 2.2.4. IL-8 release assay protocol

178 ASMCs were seeded in 0.5 ml DMEM containing 10% FBS in 48-
179 well tissue culture plates at the density of 10⁴ cells/well and grown
180 for 24 h at 37 °C with 5% CO₂. Subsequently, cells were serum
181 starved for 18 h and treated with different concentration of corti-
182 costeroids (final DMSO concentration 0.1%) for 60 min before stimu-
183 lation with TNF (0.1 ng/ml). After 18 h incubation in DMEM
184 serum free, the IL8 release in the supernatant was assayed using
185 ELISA kit (Invitrogen). Compound potencies were expressed as
186 concentration able to elicit half maximal inhibition of IL8 release
187 [IC₅₀].

188 2.2.5. Real time PCR analysis of GILZ gene expression

189 ASMCs were seeded in 0.1 ml DMEM containing 10% FBS in
190 96-well tissue culture plates at the density of 4x10³ cells/well
191 and grown for 24 h at 37 °C with 5% CO₂. Then cells were starved
192 over-night in DMEM without FBS and then treated with different
193 concentrations of compounds (10⁻¹²M–10⁻⁷M, final DMSO concen-
194 tration 0.1%) for 4 h before mRNA extraction.

195 Total RNA was isolated using TaqMan Gene expression Cells-to-
196 Ct kit (Applied Biosystems, Foster City, CA). Briefly, cells were lysed
197 in Cell Lysis solution containing DNase I for 5 min, followed by
198 two-minute incubation with the stop solution. Reverse transcrip-
199 tion reactions were performed using 10 μL of each cell lysate,
200 according to the manufacturer's instructions. Two sets of primers-
201 probes were designed for the human and rat cell lines using
202 the Primer Express Software version 3.0 (Applied Biosystems).
203 The chosen reporter fluorophores for TaqMan MGB probes were

VIC for the endogenous reference β-actin gene (ACTB) and 6-car-
204 boxylfluorescein (FAM) for GILZ or TAT genes. 205

206 The two sets of primers-probes were the follows: set 1, ACTB-
207 FW (forward) 5'-GGCGGCACCACCATGTAC-3', ACTB-RE (reverse)
208 5'-CAGGGCAGTGATCTCCTTCTG-3' ACTB probe 5'-VIC-TGGCA TTG
209 CCGACAGG-3'; set 2 GILZ-FW (forward) 5'-TGGCCATAGACAACAAG
210 ATCGA-3', GILZ-RE (reverse) 5'-TCACAGCATAATCAGATGATTC
211 TTC-3', GILZ probe 5'-FAM-AGGCCATGGATCTGG -3'. 212

213 The selected primers and probes were subjected to Basic Local
214 Alignment Search Tool (BLAST) database searches to exclude any
215 sequence similarities. Real-time quantitative PCR was performed
216 using StepOnePlus™ Real-Time PCR System (Applied Biosystems).
217 All samples were run in triplicate in a final volume of 25 μL con-
218 taining 12.5 μL of 2× TaqMan Gene Expression PCR Master Mix,
219 300 nM of each primer, 250 nM of each probe and 4 μL of RT reac-
220 tion, according to the manufacturer's instructions (Applied Biosys-
221 tems). Amplification conditions for GILZ/β-actin were: 50 °C for
222 2 min and 95 °C for 10 min, followed by 50 cycles of 95 °C for
223 30 s and 60 °C for 1 min. 224

225 Relative expression of GILZ mRNA was calculated using the
226 2-(CT) comparative method, with normalization against the inter-
227 nal endogenous reference β-actin gene. 228

229 2.2.6. Competitive binding assay

230 Competitive binding assays to evaluate the affinity of the
231 compounds to human glucocorticoid receptor and human mineral-
232 corticoid receptor were performed in triplicate in a total volume of
233 160 μL, containing 5 nM [³H]Dexamethasone or 4.5 nM [³H]
234 D-Aldosterone (Amersham Pharmacia Biotech) and various concen-
235 trations (0–1000 nM) of test compounds as previously described
236 [10]. After 24 h incubation at 4 °C, unbound [³H]Dexamethasone
237 was removed by the treatment with DCC in TEDM buffer on ice. A
238 150 μL sample was pipetted into scintillation vial and 5 ml scintilla-
239 tion cocktail were added. By using, similar assay conditions were
240 adopted for determining aldosterone binding. Non-specific binding
241 was determined in the presence of 1000-fold excess of unlabelled
242 Dexamethasone or Aldosterone respectively. The radioactivity was
243 measured with scintillation counter (Beckman Instruments, Fullerton,
244 CA). IC₅₀ values (concentrations at which 50% of specific binding
245 is displaced by the compounds) were determined from the best fit
246 lines derived by least square regression lines of competitive dis-
247 placement graph. The K_i values were calculated using the equation
248 of Cheng and Prusoff. 249

250 2.2.7. Animals

251 Male Brown Norway rats (150–200 g) and male Sprague Dawley
252 rats (250 g) were purchased from Charles River Laboratories Italy
253 (Calco, Lecco). Prior to use animals were acclimated for at least
254 5 days to the local vivarium conditions (room temperature:
255 20–24 °C; relative humidity: 40–70%), having free access to stan-
256 dard rat chow and tap water. All the procedures were performed

in animal operating rooms in conformity to the Italian legislation (D.L. vo 116/92) and the UE directive 2010/63/UE.

2.2.8. Intratracheal administration and pharmacokinetic

Compound **#15** was intratracheally administered to male Sprague Dawley rats.

Before intratracheal administration of $1 \mu\text{mol/kg}$ of **#15** as suspension at volume of 0.5 ml/kg (0.2% Tween 80 in 0.9% sodium chloride solution as vehicle) animals were anesthetized with isoflurane or sodium thiopental, in case of terminal sampling. Rats fasted from 1 h before the treatment. After i.t. treatment blood and lung were collected as follows: 0.083, 0.5, 1, 2, 4, 6, 24 and 48 h. Blood were put in heparinised plastic tubes, kept in an ice-water bath and then centrifuged within 0.5 h, for 3 min at $10,000 \times g$ at 4°C for plasma separation. Lungs were collected, washed with 10 ml of 0.9% sodium chloride solution, then frozen over liquid nitrogen. Plasma and lungs were stored at -80°C until the bioanalysis. $120 \mu\text{L}$ of plasma samples were purified adding $480 \mu\text{L}$ of acetonitrile and vortexed for 30 s., then the obtained samples were stored at -20°C for 0.5 h and centrifuged at $3600 \times g$ for 0.25 h. The supernatant was later evaporated under N_2 stream. The samples were reconstituted with $200 \mu\text{L}$ of 1% acetic acid in acetonitrile and 1% acetic acid in water mixture ($50:50, v:v$), vortexed for 30 s and injected into the LC/MS-MS system. $70 \mu\text{L}$ of homogenated lung samples, obtained adding 3 ml of saline solution and acetonitrile mixture ($50:50, v:v$) to 1 g of rat lung, were purified with $280 \mu\text{L}$ of formic acid solution (0.2% in acetonitrile) and vortexed for 30 s. then the obtained samples were stored at -20°C for 0.5 h and centrifuged at $3600 \times g$ for 0.25 h. $50 \mu\text{L}$ of an aqueous solution of formic acid solution (0.3%) were added to $150 \mu\text{L}$ of the supernatant and then vortexed for 30 s. The obtained samples ($5 \mu\text{L}$ for lung and $20 \mu\text{L}$ for plasma) were injected into the LC/MS-MS system, Thermo Electron TSQ Quantum Access, as spectrometer and Accela HPLC system. The chromatographic analysis was performed in gradient mode with Formic acid in water (0.2%) (Solvent A) and Formic acid in acetonitrile (0.2%) (Solvent B), using Accucore (Thermo Fisher) C18 ($50 \times 2.1 \text{ mM}$) $2.6 \mu\text{m}$ column equipped with a Thermo Fisher in-line filter Javelin (88200) and Accucore C18 defender guard cartridge $10 \times 2.1 \text{ mM}$, $2.6 \mu\text{m}$, operating at 40°C . The spectrometer was used in ESI positive ion mode, monitoring the following transitions: $502 \rightarrow 462$ (**#15**) and $501 \rightarrow 293$ (Fluticasone propionate, as IS).

The measured plasma concentrations were in the linear range: $0.48\text{--}533 \text{ ng/ml}$.

The measure lung concentrations properly adjusted to the corresponding weighs were in the linear range: $12.4\text{--}169680 \text{ ng/g}$.

2.2.9. Ovalbumin-induced pulmonary eosinophilia in sensitised Brown Norway rats

Male Brown-Norway rats were sensitized by intraperitoneal injection of 1 ml suspension containing ovalbumin (OVA, 1 mg/ml , Sigma Aldrich) and $\text{Al}(\text{OH})_3$ (100 mg/ml , Sigma Aldrich) for 3 consecutive days. Two weeks later the animals were nose-only exposed to an aerosol of OVA solution (1% in saline). The non challenged-vehicle-control treated animals were sensitised to OVA but exposed to aerosolized saline (sham). At 24 h after exposure either to OVA or saline aerosol, animals were anaesthetised with sevoflurane (4% in oxygen, Sevoflo, Abbott) and bronchoalveolar lavage fluid (BALF) was collected and subjected to total and differential cell counts. Cpd **#15** and Dexamethasone were administered as suspension (vehicle: saline containing 0.2% Tween 80) by the intratracheal route 2 h before and 4 h after OVA aerosol.

Data were analysed using Graph Pad Prism™. The parametric tests performed to determine statistical significance were an analysis of variance (ANOVA) with Dunnett's post-test.

2.3. Modelling studies

The crystal structure of Dexamethasone in complex with human GR was retrieved from Brookhaven Protein Databank (PDB code: 1M2Z) [11] and utilized for binding site analysis using SiteMap (Schrodinger9.1) and for docking studies using GlideSP (Schrodinger9.1) [12].

Finally, logP and pKa values were calculated with the use of ACD/Labs (v12) [13].

3. Results

3.1. Chemistry

A series of isoxazolines, **Cpds #1–18** described in Table 1, was prepared following the synthetic pathway summarized in Scheme 1.

Intermediates $11\beta,21$ -dihydroxy-pregna-1,4,16-triene-3,20-dione (intermediate **#19**) and $6,9$ -difluoro- $11\beta,21$ -dihydroxy-pregna-1,4,16-triene-3,20-dione (intermediate **#20**) were prepared respectively in four and two steps starting from commercially available Prednisone 21-O-acetate and Difluprednate by a method established in this laboratory [14]. For example, 1,3-dipolar cycloaddition of 4-chlorophenylformonitrile oxide (generated *in situ* by the treatment of 4-chloro-N-hydroxybenzimidoyl chloride with aqueous NaHCO_3 solution) [15] to an α,β -unsaturated enone **#19** gave a single adduct **#1** in a good yield. Only the 16,17-double bond reacted with the various nitrile oxides and ^1H NMR spectra are consistent with the proposed structures. The regioselectivity of 1,3-dipolar cycloaddition of nitrile oxides to an α,β -unsaturated enone and the stereospecificity of the cycloaddition to 16-ene steroid system are known [16,17].

3.2. In vitro and in vivo evaluation of novel isoxazolines derivatives

3.2.1. GR binding affinity

The affinity for the human GR receptor of this novel series of isoxazolines was measured in a binding assay and compared with Dexamethasone and Deflazacort as reference ligands. As reported in Table 2, the great majority of the compounds exhibited K_i values between 0.5 and 250 nM. In particular, the bromine derivative Cpd **#15** showed the lowest K_i value (0.5 nM).

3.2.2. GR nuclear translocation

The potency and efficacy of the isoxazoline derivatives in inducing nuclear translocation were evaluated in an enzyme fragment complementation format by using CHO-K1 PathHunters™ cells [18]. As reported in Table 2, EC_{50} s values lie between 9 and 884 nM. In particular, the bromine derivative Cpd **#15** stands out as the most potent derivative in this assay with an EC_{50} value of 9 nM, while Dexamethasone showed an EC_{50} value of 25 nM (Table 2 and Fig. 1).

3.2.3. Effect of varying concentrations of isoxazolines compounds on the LPS-evoked NO release in RAW 264.7

RAW 264.7 is a murine cell line of immortalized peritoneal macrophages which has been widely used for studying inflammatory responses in macrophages. In particular, LPS-evoked nitric oxide (NO) release is an index of inflammatory activation in these cells.

RAW264.7 were stimulated for 24 h with LPS (100 ng/ml) after 1 h pre-incubation with different concentrations of compounds tested ($0.01\text{--}1000 \text{ nM}$).

Among the isoxazolines tested, **Cpd #6**, **Cpd #9**, **Cpd #14** and **Cpd #15** showed to be more potent or equipotent to

Table 2
In vitro data.

Compound	K _i [nM] ^a	GR translocation EC ₅₀ [nM]	% Efficacy vs. dexamethasone	RAW NO ^b release IC ₅₀ (nM)
#1	107.3	161.7	16	c
#2	84.2	884.8	32	c
#3	1630.8	327	21	c
#4	249.5	c	–	c
#5	85.2	236.2	22	c
#6	66.6	212.4	41	135
#7	9.4	192.3	52	c
#8	55.3	272	25	c
#9	2.5	22.6	67	69.4
#10	>10000	c	–	c
#11	31.7	126.3	29	c
#12	59.7	243.9	28	c
#13	2.4	68.6	80	c
#14	3.2	56.4	66	53.7
#15	0.5	9.0	91	6.1
#16	1.5	129.4	76	–
#17	3.0	48.8	40	–
#18	2.5	22.9	42	–
Deflazacort ^d	10.8	–	–	–
Dexamethasone	2.3	25	100	115

^a Concentration displacing 50% of GR bound [³H]Dexamethasone values represent the mean of at least two experiments. The standard deviation of the mean of GR K_i is ≤18%.

^b Order of magnitude: –9.

^c No inhibition up to 1 μM.

^d The des-acetyl-derivative.

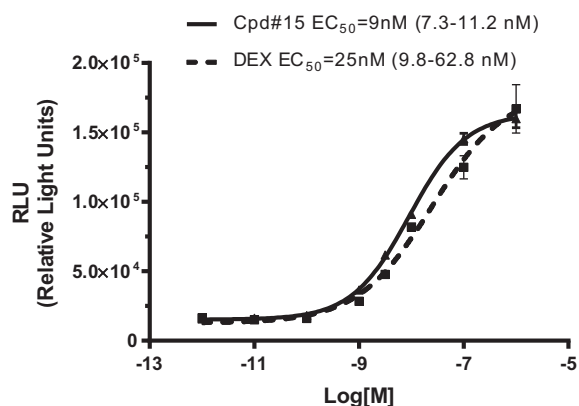


Fig. 1. Steroid-evoked stimulation of GR nuclear translocation. Concentration-response curves in CHO-K1 PathHunter™ cells incubated with Dexamethasone (DEX) or **Cpd #15** for 3 hrs. Data shown are mean ± SD of a representative experiment performed in triplicate.

dexamethasone in inhibiting LPS-induced NO release from RAW264.7, whereas the other compounds tested exhibited poor inhibitory activity against NO release (IC₅₀ > 1 μM) (Table 2, Fig. 2).

3.2.4. MR nuclear translocation

The human mineralocorticoid receptor (MR) is highly homologous to GR [19,20]. In order to determine receptor selectivity, **Cpd #15** was tested in a competitive binding assay and in a MR nuclear translocation functional assay head to head with aldosterone and dexamethasone.

Cpd #15 and dexamethasone showed a K_i for the mineralocorticoid receptor of 45.0 nM (c.i. 28–74) and 12.5 nM (c.i. 5.3–30.6) respectively.

As reported in Table 3, **Cpd #15** showed potency and efficacy in eliciting MR translocation greatly inferior to aldosterone and similar to Dexamethasone (Fig. 3). The same experimental set up was

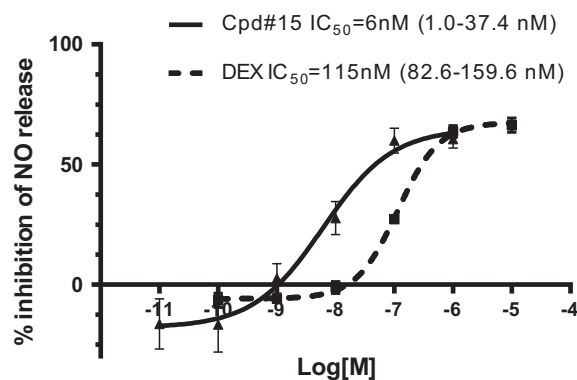


Fig. 2. Inhibitory effect of increasing concentrations of corticosteroids isoxazolines on the accumulation of nitrite induced by LPS. Concentration-dependent inhibition by Dexamethasone (DEX) and **Cpd #15** of LPS-evoked NO release in Raw 264.7 cells. Each data point is the mean ± SD of a representative experiment performed in triplicate.

Table 3
Mineralocorticoid receptor nuclear translocation.

Compound	EC ₅₀ [nM]	% Efficacy vs. aldosterone
#9	37.6	20
#13	76.5	30
#14	66.6	19
#15	6.1	50
Dexamethasone	9.2	50

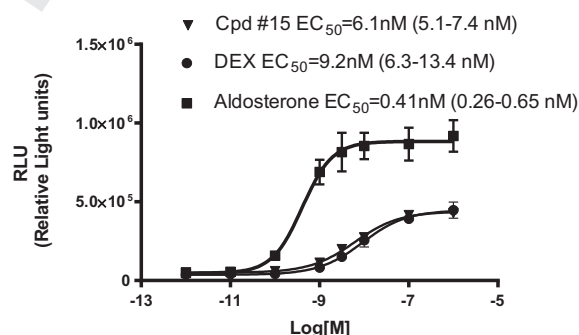


Fig. 3. Steroid-evoked stimulation of MR nuclear translocation. Concentration-response curves in CHO-K1 PathHunter™ cells incubated with Dexamethasone (DEX), **Cpd #15** and Aldosterone for 3 hrs. Data are mean ± SD of a representative experiment performed in triplicate.

run with cell culture medium containing charcoal stripped fetal bovine serum to delete cortisol, that could be present in cell culture medium. Indeed, results comparable to the non-stripped serum condition were obtained: EC₅₀ = 7.2 nM (c.i. 6.8–7.6) for **Cpd #15** and EC₅₀ = 7.5 nM (c.i. 7.2–7.7) for dexamethasone. **Cpd #9**, **#13**, **#14** tested in the MR translocation assay appeared to be 4–7-fold less potent than **Cpd #15**.

3.2.5. Effect of varying concentrations of isoxazoline compound **Cpd #15** on the TNFα-evoked IL-8 release in ASMCs

In the airways smooth muscle cells (ASMCs) the secretion of IL-8 induced by inflammatory mediators is repressed by glucocorticoids [21] through a direct inhibitory interaction of the GR with activated transcription factors, such as NF-κB and AP-1 [22].

The anti-inflammatory effects of novel isoxazoline **Cpd #15** was assessed by measuring its potency in inhibiting TNFα-induced IL-8 release in ASMCs. As shown in Fig. 4, **Cpd #15** inhibited IL-8 release

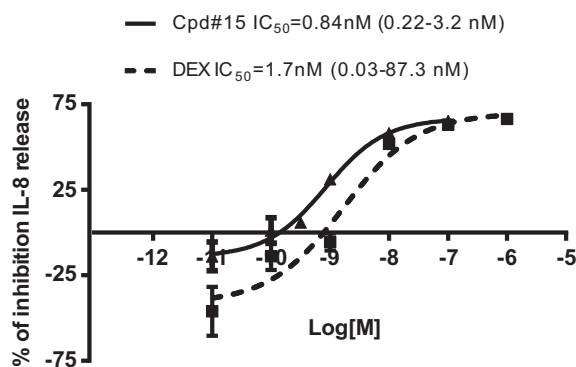


Fig. 4. Inhibitory effect of increasing concentrations of corticosteroids isoxazolines on IL-8 release induced by TNF α . Concentration-dependent inhibition by Dexamethasone (DEX) and **Cpd #15** of TNF α (0.1 ng/ml)-evoked IL-8 release in ASMCs. Data are mean \pm SD of a representative experiment performed in triplicate.

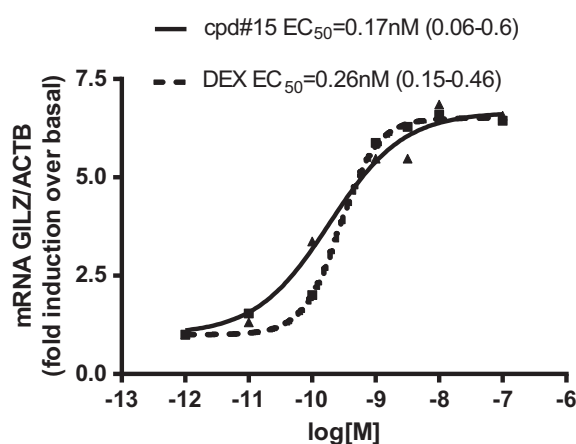


Fig. 5. Dose–response curves for reference compounds Dexamethasone (DEX) and isoxazoline **Cpd #15** on mRNA GILZ induction in airway smooth muscle cells. Relative GILZ mRNA levels were measured by Taqman real-time PCR and normalized to β actin. Data are mean \pm SD of a representative experiment performed in triplicate.

with a sub-nanomolar potency ($EC_{50} = 0.84$ nM) comparable to that of Dexamethasone ($EC_{50} = 1.7$ nM).

3.2.6. **Cpd #15** induces transactivation of the anti-inflammatory gene GILZ in human airway smooth muscle cells

Part of the anti-inflammatory properties of glucocorticoids depend also on their ability to trans-activate genes able to counteract inflammatory processes such as GC-induced leucine zipper (GILZ) [23].

Following incubation of ASMCs with increasing concentration of **Cpd #15** or Dexamethasone, relative GILZ mRNA amounts were measured by TaqMan real-time PCR and normalized with respect to β -actin. As shown in Fig. 5, **Cpd #15** displayed a potency ($EC_{50} = 0.17$ nM) and efficacy in inducing GILZ mRNA (about 6-fold induction over basal) comparable to those of Dexamethasone.

Table 4
PK data of **Cpd #15**.

	C_{max} (nmol/ml or nmol/g)	AUC_{last} (nmol/ml \cdot h or nmol/g \cdot h)	$T_{1/2}$ (h)	T_{last} (h)	MRT_{last} (h)
Plasma (i.t.)	0.448	0.232	1.59	6	1.09
Lung (i.t.)	55.37	147.78	6.47	24	5.35

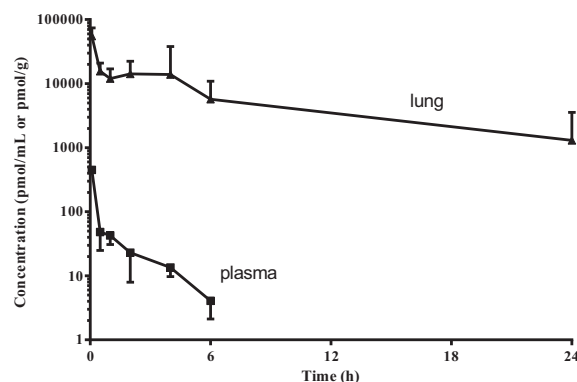


Fig. 6. Plasma (squares) and lung (triangles) levels after i.t. administration of **Cpd #15** (1 μ mol/kg) to rats.

3.2.7. *In vitro* ADME and PK profile

Cpd #15 showed a medium rate of clearance in rat hepatocytes (25.8 μ L/min 10^6 cells) and was stable in rat plasma (up to 5 h) as well as in S9 lung homogenates (45% after 1 h).

Following intra-tracheal (i.t.) administration in rat, **Cpd #15** (1 μ mol/kg) showed a C_{max} value of 0.448 nmol/ml in plasma and the exposure achieved was 0.232 nmol/ml \cdot h. In the lung, **Cpd #15** levels peaked at 0.083 h reaching a concentration of 55.37 nmol/g and its exposure (AUC_{last}) was 147.78 nmol/g \cdot h, with a MRT_{last} of 5.35 h (Table 4). (See Fig. 6)

3.2.8. Effect of #15 on OVA-induced eosinophilia in sensitised Brown Norway rats

The effects of **Cpd #15** and the reference compound Dexamethasone in a rat model of asthma (OVA-induced pulmonary eosinophilia) were investigated. Animals were dosed i.t. with **Cpd #15** (0.1 – 1 μ mol/kg) or Dexamethasone (1 μ mol/kg) 2 h prior to and 4 h post OVA challenge.

Cpd #15 inhibited the OVA-induced increase in eosinophil number in the BAL in a dose-dependent fashion (Fig. 7). The inhibitory responses ranged from 43% (0.1 μ mol/kg) to 95% (1 and 3 μ mol/kg) and were statistically significant ($p < 0.05$ – $p < 0.01$) at all tested doses. The inhibitory effect of 1 μ mol/kg Dexamethasone was superimposable to that of 1 μ mol/kg of **Cpd #15**.

3.3. Modelling studies

Overlay of **Cpd #15** (GlideSP docked conformation) on Dexamethasone bound to the ligand binding domain of human GR is shown in Fig. 8. The contour map highlights that the steroid binding site is mainly hydrophobic (yellow grids). An extended polar region is located near R611 and N570 both involved in hydrogen bond interactions with the 3 – C = O of Dexamethasone. Besides, a small polar area (red and blue grids) is close to N564 which is involved in a hydrogen bond interaction with 11-OH of the ligand. Finally, the hydroxyl moiety of Dexamethasone at C17 is nicely accommodated in a polar pocket and makes a hydrogen bond interaction with Q642.

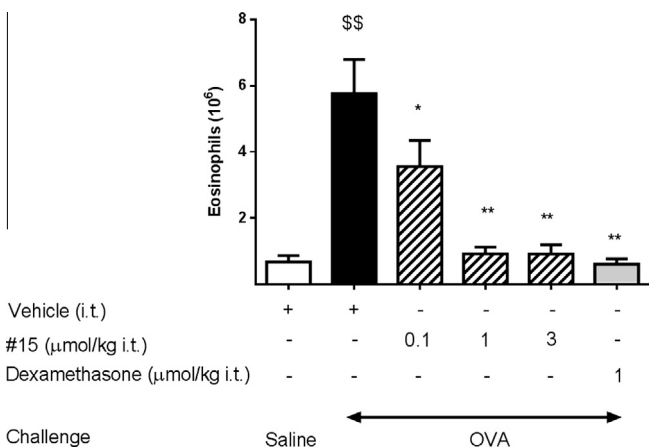


Fig. 7. Compound #15 dose–response curve in the rat model of OVA-induced eosinophilia. Test compounds were administered i.t. to sensitized Brown Norway rats 2 h before and 4 h after OVA challenge. Each column represents the mean of total eosinophil number in BAL and each bar represents SEM. Changes were compared to the OVA challenged group (*) or to the sham challenged group (\$) using ANOVA followed by Dunnett's test. * $p < 0.05$ and ** $p < 0.01$, \$\$\$ $p < 0.01$, $n = 6$ –7 animals/group.

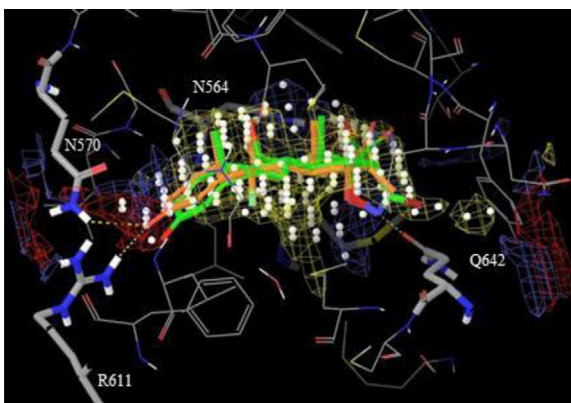


Fig. 8. Overlay of a docking solution of Cpd #15 on the X-ray structure of Dexamethasone (orange) bound to the ligand binding domain of human GR (1MZZ PDB code) [11] (For interpretation of the references to colour in this figure legend, the reader is referred to the web version of this article.)

4. Discussion

4.1. SAR interpretation

Cpd #7 ($K_i = 22.33$ nM) shows a comparable binding affinity to the active metabolite of Deflazacort (see [Chart 1](#), $K_i = 10.84$ nM). Small alkyl substituents are preferred at the C3' position for the binding affinity. In particular, C3'-methyl-isoxazoline derivative shows better binding affinity than C3'-n-propyl-isoxazoline derivative **Cpd #6** ($K_i = 66.59$ nM). When the methyl group is replaced with a hydroxyl-methyl moiety, as in **Cpd #8**, the affinity is reduced ($K_i = 55.29$ nM), which suggests that polar groups are not tolerated. This is further confirmed by the lack of activity of **Cpd #10** ($K_i = > 10,000$). Improved affinity is obtained if the isoxazoline ring is decorated with a bromine at C3' as in **Cpd #9** ($K_i = 2.46$ nM).

The inhibitory effect of compounds with R equal to hydrogen (see [Scheme 1](#)) on NO production in RAW 264.7 macrophage cells, described in Park et al. [5], is 10-fold lower than Cpd #15.

In order to expand the SAR of new chemical series, aromatic and heterocyclic moieties were introduced. The unsubstituted phenyl

ring with X, Y equal to hydrogen showed very weak potency and efficacy in the Raw assay and was not further profiled (unpublished results). **Cpd #1**, bearing a p-chlorophenyl substituent at C3' on the isoxazoline ring at the C16–17 position, displays only moderate binding affinity ($K_i = 262.96$ nM). Substitution of the p-chlorine moiety with p-methoxy group on the phenyl ring at C3', as in **Cpd #4** ($K_i = 249.54$ nM) slightly improves the affinity in the binding assay. Replacement of the phenyl ring with either a furyl, **Cpd #12**, or a thienyl, **Cpd #11**, did not improve the affinity at GR ($K_i = 59.66$ and 31.73 respectively).

The relatively weak GR binding affinity of the compounds with X, Y = Hydrogen was improved with the incorporation of two fluorine atoms at C6, C9 on the corticosteroid core. These isoxazoline derivatives showed a 10-fold increase in their binding affinity while their potency did not change significantly.

The increase of the size and bulk of the para-substituent of phenyl derivative led to a reduction in both potency and efficacy in the GR nuclear translocation, e.g., **Cpd #18**.

These results were rationalized in light of the binding modes of this compound series by using docking methods. As shown in [Fig. 8](#), the isoxazolidine ring of **Cpd #15** maps well the same polar region filled by the hydroxyl moiety at C20 of Dexamethasone, while the bromine substituent is nicely accommodated in a small hydrophobic pocket. The limited size of this cavity highlighted by the yellow grid map suggests that bulkier groups like phenyl (**Cpd #18**), thienyl (**Cpd #11**) and furyl (**Cpd #14**) are not tolerated due to their large steric hindrance which can be described with the use of calculated Molecular Refractivity (MR) parameter [24]. Mapping of this pocket appears to be suitable for small and hydrophobic substituents such as Br (**Cpd #9** and **Cpd #15**) and Me (**Cpd #7**). Both are characterized by low MR values (Br: $MR = 8.88$; Me: $MR = 5.65$) and medium lipophilicity (Br: $cLogP = 1.73$; Me: $cLogP = 2.53$) [14]. When either steric bulk or polarity increases, binding affinity significantly drops as observed for **Cpd #6** (R = propyl: $MR = 14.96$, $cLogP = 3.55$), **Cpd #8** (R = CH_2OH : $MR = 7.19$, $cLogP = 1.38$) and **Cpd #2** (R = $COOEt$: $MR = 17.47$, $cLogP = 1.45$) and is completely lost for **Cpd #3** which is likely charged at physiological pH (calculated $pK_a = 2.74$).

4.2. Biological profile Cpd #15

The most interesting compound among the novel isoxazoline derivatives, described in this study, is the bromine derivative **Cpd #15**, which proved to be the most potent compound in the GR binding assay and in the cell-based GR nuclear translocation assay. **Cpd #15** showed K_i values pointing out a 50-fold higher affinity for GR vs. MR in the binding assay. The K_i ratio between MR and GR for dexamethasone is about 5, suggesting that **Cpd #15** is relatively more selective than dexamethasone. The observation that **Cpd #15** interaction with MR is also associated with nuclear translocation, suggests that such compound acts as an agonist at the MR. In order to evaluate its anti-inflammatory potency, we examined the effects on the release of relevant inflammatory mediators. **Cpd #15** dose-dependently inhibited the production of nitric oxide in LPS-stimulated Raw 264.7 macrophages, with a potency superior to the reference compound Dexamethasone. Inhibition of nitric oxide release in Raw 264.7 macrophages occur with relatively high EC_{50} with respect to K_i values due likely to the mechanism of suppression that requires transcriptional and post-transcriptional down regulation of the enzyme nitric oxide synthase [25]. It should also be kept in mind that Raw 264.7 are immortalized cell lines which are known to express relatively high levels of P-glycoproteins [26]. Upregulation of P-glycoprotein may cause drug resistance as well as reduced glucocorticosteroid responsiveness [27]. On the other hand, the repression of inflammatory responses by glucocorticoids also involves the up-regulation of anti-inflammatory genes,

including GILZ, whose expression is up-regulated by steroids in several cellular type including smooth muscle cells [28]. In human ASMCs, **Cpd #15** evoked a significant concentration-dependent induction of GILZ expression and suppression of TNF α -stimulated production of IL-8 with a potency and efficacy comparable to dexamethasone. In both assays, **Cpd #15** and dexamethasone show sub/low nanomolar EC₅₀ values close to respective Ki values.

Having demonstrated that **Cpd #15** is a potent anti-inflammatory agent *in vitro*, and that its pharmacokinetic profile is suitable for topical administration (pulmonary levels > 100-fold higher than plasma levels upon *i.t.* delivery), we tested it in an *in vivo* model of allergen-induced pulmonary inflammation. Ovalbumin (OVA) inhalation to sensitized rats is a well characterized and recognized model for asthma [29]. This model is commonly used to investigate the anti-inflammatory activity of compounds developed for the treatment of allergic inflammatory airway diseases, such as corticosteroids and phosphodiesterase 4 (PDE4) inhibitors [30–32]. **Cpd #15**, when administered via the intratracheal route, proved to be as efficacious as Dexamethasone in counteracting eosinophilic infiltration in the broncho-alveolar lavage following OVA challenge (ED₅₀ < 0.3 μ mol/kg).

In conclusion, through a rational drug design approach we identified **Cpd #15**, a novel isoxazoline with a potent and robust anti-inflammatory profile which exhibits a pharmacokinetic and pharmacodynamic profile suitable for topical pulmonary delivery.

Therefore, **Cpd #15** could potentially be developed as an inhalable agent for the treating of pulmonary inflammation such as asthma and COPD.

Acknowledgments

We kindly thank Mr. Pier Tonino Bolzoni (Chiesi Farmaceutici, Parma, Italy) for skilful technical support.

Appendix A. Supplementary data

Supplementary data associated with this article can be found, in the online version, at <http://dx.doi.org/10.1016/j.steroids.2014.12.016>.

References

- [1] Stanbury RM, Graham EM. Systemic corticosteroid therapy-side effects and their management. *Br J Ophthalmol* 1998;82:704–8.
- [2] Barnes NC. The properties of inhaled corticosteroids: similarities and differences. *Prim Care Respir J* 2007;16:149–54.
- [3] Ernst P, Suissa S. Systemic effects of inhaled corticosteroids. *Curr Opin Pulm Med* 2012;18:85–9.
- [4] Kwon T, Heiman AS, Oriaku ET, Yoon K, Lee HJ. New steroidal anti-inflammatory antedugs: steroidal [16,17-d]-3-carbomethoxyisoxazolines. *J Med Chem* 1995;38:1048–51.
- [5] Kwan-k Park, Dong-H Ko, You Z, Omar M, Khan F, Lee HJ. *In vitro* anti-inflammatory activities of new steroidal antedugs: [16 α ,17 α -d] isoxazoline and [16 α ,17 α -d]-3-hydroxy-iminoformyl isoxazoline derivatives of prednisolone and 9 α -fluoroprednisolone. *Steroids* 2006;71:183–8.
- [6] Kanemasa S, Matsuda H, Kamimura A, Kakinami T. *Tetrahedron* 2000;56:1057–64.
- [7] Kwon T, Heiman AS, Oriaku ET, Yoon K, Lee HJ. *J Med Chem* 1995;38:1048–51; Bacher E, Demnitz FWJ, Hurni T. *Tetrahedron* 1997;53(42):14317–26.

- [8] Yuan L; Yanchang L; Jinlu L; Chaohui S CN 101177443 A 20080514.
- [9] Fung P, Peng K, Kobel P, Dotimas H, Kauffman L. A homogeneous cell-based assay to measure nuclear translocation using beta-galactosidase enzyme fragment complementation. *Assay Drug Dev Technol* 2006;4:263–72.
- [10] Wambach G, Casals-Stenzel J. Structure-activity relationship of new steroidal aldosterone antagonists. Comparison of the affinity for mineralocorticoid receptors *in vitro* and the antialdosterone activity *in vivo*. *Biochem Pharmacol* 1983;32:1479–85; Mulatero P, Panarelli M, Schiavone D, Rossi A, Mengozzi G, Kenyon CJ. Impaired cortisol binding to glucocorticoid receptors in hypertensive patients. *Hypertension* 1997 Nov;30(5):1274–8.
- [11] Bledsoe RK, Montana VG, Stanley TB, Delves CJ, Apolito CJ, McKee DD. Crystal structure of the glucocorticoid receptor ligand binding domain reveals a novel mode of receptor dimerization and coactivator recognition. *Cell* 2002 Jul 12;110(1):93–105.
- [12] [Schrödinger, Maestro version 9.1 Schrödinger, LLC, New York 2009 <http://www.schrodinger.com/>].
- [13] ACD/LogP v12, www.acdlabs.com.
- [14] Armani E, Ghidini E, Peretto I, Virdis A. Isoxazolidine derivatives WO 2011/029547 A8.
- [15] Mukaiyama T, Hoshino T. The reactions of primary nitroparaffins with isocyanates. *J Am Chem Soc* 1960;2:5339–42.
- [16] Moersch GW, Wittle EL, Neuklis WA. The decarboxylation of 3-carboxy-2-isoxazolines. 3 β ,17 α -dihydroxypregna-5-en-20-one-16 α -carbonitrile. *J Org Chem* 1967;32:1387–91.
- [17] Moersch GW, Wittle EL, Neuklis WA. The decarboxylation of 3-carboxy-2-isoxazolines. *J Org Chem* 1966;30:1272–3.
- [18] Plumb J, Robinson L, Lea S, Banyard A, Blaikley J, Ray D. Evaluation of glucocorticoid receptor function in COPD lung macrophages using beclomethasone-17-monopropionate. *PLoS One* 2013;8:e64257.
- [19] Pippal JB, Fuller PJ. Structure-function relationships in the mineralocorticoid receptor. *J Mol Endocrinol* 2008;41:405–13.
- [20] Fuller PJ, Yao Y, Yang J, Young MJ. Mechanisms of ligand specificity of the mineralocorticoid receptor. *J Endocrinol* 2012;213:15–24.
- [21] John M, Au BT, Jose PJ, Lim S, Saunders M, Barnes PJ. Expression and release of interleukin-8 by human airway smooth muscle cells: inhibition by Th-2 cytokines and corticosteroids. *Am J Resp Cell Mol* 1998;18:84–90.
- [22] King EM, Holden NS, Gong W, Rider CF, Newton R. Inhibition of NF-kB-dependent transcription by MKP-1. *J. Biol. Chem.* 2009;284:26803–15.
- [23] Ayroldi E, Riccardi C. Glucocorticoid-induced leucine zipper (GILZ): a new important mediator of glucocorticoid action. *FASEB J* 2009;23(11):3649–58.
- [24] Tabulated MR parameters for aromatic ring substituents were retrieved from the following papers Hansch et al. *J Med Chem* 1973;16(11):1208; Skagerberg B et al. *Quant Struct Act Relat* 1989;8:32–8.
- [25] Söderberg M, Raffalli-Mathieu F, Lang MA. Regulation of the murine inducible nitric oxide synthase gene by dexamethasone involves a heterogeneous nuclear ribonucleoprotein I (hnRNPI) dependent pathway. *Mol Immunol* 2007;44(12):3204–10.
- [26] Roy KR, Arunasree KM, Dhoot A, Aparna R, Reddy GV, Vali S. C-Phycocyanin inhibits 2-acetylaminofluorene-induced expression of MDR1 in mouse macrophage cells: ROS mediated pathway determined via combination of experimental and *in silico* analysis. *Arch Biochem Biophys* 2007;459(2):169–77.
- [27] Montano E, Schmitz M, Blaser K, Simon HU. P-glycoprotein expression in circulating blood leukocytes of patients with steroid-resistant asthma. *J Investig Allergol Clin Immunol* 1996;6(1):14–21.
- [28] Kelly MM, King EM, Rider CF, Gwozd C, Holden NS, Eddleston J. Corticosteroid-induced gene expression in allergen-challenged asthmatic subjects taking inhaled budesonide. *Br. J. Pharmacol.* 2012;165:1737–47.
- [29] Leung SY, Williams AS, Nath P, Dinh QT, Oates T, Blanc FX. Dose-dependent inhibition of allergic inflammation and bronchial hyperresponsiveness by budesonide in ovalbumin-sensitized Brown-Norway rats. *Pulm Pharmacol Ther* 2008;21:98–104.
- [30] Huang TJ, Eynott P, Salmon M, Nicklin PL, Chung KF. Effect of topical immunomodulators on acute allergen inflammation and bronchial hyperresponsiveness in sensitised rats. *Eur J Pharmacol* 2002;437:187–94.
- [31] Wollin L, Bundschuh DS, Wohlsen A, Marx D, Beume R. Inhibition of airway hyperresponsiveness and pulmonary inflammation by roflumilast and other PDE4 inhibitors. *Pulm Pharmacol Ther* 2006;19:343–52.
- [32] Chapman RW, House A, Richard J, Prelusky D, Lamca J, Wang P. Pharmacology of a potent and selective inhibitor of PDE4 for inhaled administration. *Eur J Pharmacol* 2010;643:274–81.

589
590
591
592
593
594
595
596
597
598
599
600
601
602
603
604
605
606
607
608
609
610
611
612
613
614
615
616
617
618
619
620
621
622
623
624
625
626
627
628
629
630
631
632
633
634
635
636
637
638
639
640
641
642
643
644
645
646
647
648
649
650
651
652
653
654
655
656
657
658
659
660
661